Bromine as a Partial Oxidant. Oxidation State and Charge Transport in Brominated Nickel and Palladium Bis(diphenylglyoximates). A Comparison with the Iodinated Materials and Resonance Raman Structure–Spectra Correlation for Polybromides

Davida W. Kalina,[1a] **Joseph W. Lyding,**[1b] **Mark T. Ratajack,**[1b] **Carl R. Kannewurf,**[*1b] **and Tobin J. Marks*[1a,c]**

Contribution from the Department of Chemistry, the Department of Electrical Engineering and Computer Science, and the Materials Research Center, Northwestern University, Evanston, Illinois 60201. Received January 21, 1980

Abstract: This paper presents an investigation of oxidation state and charge transport in the low-dimensional materials $Ni(dpg)_2Br_{1.0}$ and $Pd(dpg)_2Br_{1.1}$, dpg = diphenylglyoximato. Resonance Raman structure–spectra correlations are discussed for polybromides, and Br_5^- is assigned as the predominant halogen species in both of these materials. Thus, the $M(dpg)_2$ units are formally in fractional oxidation states of ca. +0.20 (2) (M = Ni) and +0.22 (2) (M = Pd). In the optical spectra of both materials, a broad transition at 500 nm is related to the polybromide chains. Four-probe single crystal electrical conductivities (dc) in the stacking direction at 300 K are as high as 9.1×10^{-4} (Ω cm)$^{-1}$ ($Ni(dpg)_2Br_{1.0}$) and 1.5×10^{-4} (Ω cm)$^{-1}$ ($Pd(dpg)_2Br_{1.1}$). The conductivity is demonstrated to be thermally activated with activation energies of 0.33 and 0.21 eV, respectively. The transport properties of the brominated materials are found to be very similar to those of the related $M(dpg)_2I$ materials (M = Ni, Pd), a result contrary to expectations if the halogen chains were the major charge carrier.

Solids exhibiting unusual low-dimensional, supermolecular cooperative phenomena have been the subject of intensive investigation in the past few years.[2] Concurrent emphasis has been placed upon developing rational synthetic routes to new materials and upon developing the theoretical models needed to understand existing data as well as to guide future experiments. One successful approach to the synthesis of unidimensional, quasi-metallic materials has been the partial oxidation by iodine[2,3] of stackable, conjugated, planar molecules having a certain selected range of ionization potentials.[3a] A rich variety of conductive mixed-valent materials have been prepared from metallomacrocyclic precursors such as bis(diphenylglyoximates),[3,4] phthalocyanines,[3,5] dibenzotetraazaannulenes,[6] bis(benzoquinonedioximates),[3,7] and porphyrins;[8] highly conductive halogenated organic systems have included those derived from organochalcogenides such as tetrathiafulvalene[3,9] and tetrathiatetracene.[10,11] The structures of these types of materials invariably consist of stacks of mixed-valent (partially oxidized) electron donors and chains of electron-accepting iodide or polyiodide counterions.[3a] A particular strength of the iodine oxidation procedure is that the form of the iodine (even if disordered) can be readily deduced from resonance Raman and iodine Mössbauer structure–spectra criteria.[3,12] Hence, if the stoichiometry is known, the actual degree of incomplete charge transfer can be readily determined.

(1) (a) Department of Chemistry and the Materials Research Center. (b) Department of Electrical Engineering and Computer Science, and the Materials Research Center. (c) Camille and Henry Dreyfus Teacher-Scholar.

(2) (a) "Highly Conductive One-Dimensional Solids", Devreese, J. T., Evrard, V. E., Van Doren, V. E., Eds.; Plenum Press: New York, 1979. (b) Torrance, J. B. *Acc. Chem. Res.* **1979**, *12*, 79–86. (c) Miller, J. S., Epstein, A. J., Eds. *Ann. N.Y. Acad. Sci.* **1978**, *313.* (d) Keller, H. J., Ed. *NATO Adv. Study Inst. Ser., Ser. B* **1977**, *25.* (e) Miller, J. S.; Epstein, A. J. *Prog. Inorg. Chem.* **1976**, *20*, 1–151. (f) Keller, H. J., Ed. *Nato Adv. Study Inst. Ser., Ser. B*, **1977**, *7.* (g) Soos, Z. G.; Klein, D. J. In "Molecular Associations"; Foster, R., Ed.; Academic Press, New York, 1975; Chapter 1.

(3) (a) Marks, T. J.; Kalina, D. W. In "Extended Linear Chain Compounds"; Miller, J. S., Ed., Plenum Press: New York, in press. (b) Marks, T. J. *Ann. N.Y. Acad. Sci.* **1978**, *313*, 594–616.

(4) (a) Cowie, M. A.; Gleizes, A.; Grynkewich, G. W.; Kalina, D. W.; McClure, M. S.; Scaringe, R. P.; Teitelbaum, R. C.; Ruby, S. L.; Ibers, J. A.; Kannewurf, C. R.; Marks, T. J. *J. Am. Chem. Soc.* **1979**, *101*, 2921–2936, and references therein. (b) Miller, J. S.; Griffiths, C. H. *Ibid.* **1977**, *99*, 749–755. (c) Gleizes, A.; Marks, T. J.; Ibers, J. A. *Ibid.* **1975**, *97*, 3545–3546.

(5) (a) Petersen, J. L.; Schramm, C. S.; Stojakovic, D. R.; Hoffman, B. M.; Marks, T. J. *J. Am. Chem. Soc.* **1977**, *99*, 286–288. (b) Schramm, C. S.; Stojakovic, D. R.; Hoffman, B. M.; Marks, T. J. *Science (Washington, D.C.)* **1978**, *200*, 47–48. (c) Scaringe, R. P.; Schramm, C. J.; Stojakovic, D. R.; Hoffman, B. M.; Ibers, J. A.; Marks, T. J. *J. Am. Chem. Soc.*, in press. (d) Schoch, K. F., Jr.; Kundalkar, B. R.; Marks, T. J. *Ibid.* **1979**, *101*, 7071–7073. (e) Marks, T. J.; Schoch, K. F., Jr.; Kundalkar, B. R. *Synth. Met.* **1980**, *1*, 337–347. (f) Dirk, C. W.; Lyding, J. W.; Schoch, K. F., Jr.; Kannewurf, C. R.; Marks, T. J. *Org. Coatings Plastics Chem.*, **1980**, *43*, 646–651. (g) Dirk, C. W.; Mintz, E. A.; Schoch, K. F., Jr.; Marks, T. J. *J. Macromol. Sci.-Chem.*, in press.

(6) (a) Lin, L.-S.; McClure, M. S.; Lyding, J. W.; Ratajack, M. T.; Wang, T.-C.; Kannewurf, C. R.; Marks, T. J. *J. Chem. Soc., Chem. Commun.*, in press. (b) McClure, M. S.; Lin, L.-S.; Whang, T.-C.; Ratajack, M. T.; Kannewurf, C. R.; Marks, T. J. *Bull. Am. Phys. Soc.* **1980**, *25*, 315.

(7) (a) Brown, L. D.; Kalina, D. W.; McClure, M. S.; Ruby, S. L.; Schultz, S.; Ibers, J. A.; Kannewurf, C. R.; Marks, T. J. *J. Am. Chem. Soc.* **1979**, *101*, 2937–2946. (b) Marks, T. J.; Webster, D. F.; Ruby, S. L.; Schultz, S. *J. Chem. Soc., Chem. Commun.* **1976**, 444–445. (c) Endres, H.; Keller, H. J.; Megnamisi-Bélombé, M.; Moroni, W.; Nöthe, D. *Inorg. Nucl. Chem. Lett.* **1974**, *10*, 467–471. (d) Endres, H.; Keller, H. J.; Moroni, W.; Weiss, J. *Acta Crystallogr., Sect. B* **1975**, *B31*, 2357–2358. (e) Endres, H.; Keller, H. J.; Megnamisi-Bélombé, M.; Moroni, W.; Pritzkow, H.; Weiss, J.; Comes, R. *Acta Crystallogr., Sect. A* **1976**, *A32*, 954–957.

(8) Phillips, T. E.; Scaringe, R. P.; Hoffman, B. M.; Ibers, J. A. *J. Am. Chem. Soc.* **1980**, *102*, 3435–3444.

(9) (a) Teitelbaum, R. C.; Johnson, C. K.; Marks, T. J. *J. Am. Chem. Soc.* **1980**, *102*, 2986–2989, and references therein. (b) Somoano, R. B.; Gupta, A.; Hadek, V.; Datta, T.; Jones, M.; Deck, R.; Hermann, A. M. *J. Chem. Phys.* **1975**, *63*, 4970–4976. (c) Warmack, R. J.; Callcott, T. A.; Watson, C. R. *Phys. Rev. B: Solid State* **1975**, *12*, 3336–3338. (d) Scott, B. A.; LaPlaca, S. J.; Torrance, J. B.; Silverman, B. D.; Welber, B. *J. Am. Chem. Soc.* **1977**, *99*, 6631–6639, and references therein. (e) Johnson, C. K.; Watson, C. R., Jr.; Warmack, R. J. "Abstracts", 25th Meeting of the American Crystallographic Association; 1975; SC6, p 19. (f) Johnson, C. K.; Watson, C. R., Jr.; Warmack, R. J. *Annu. Prog. Rep.-Oak Ridge Natl. Lab., Chem. Div.* **1976**, 102–103.

(10) (a) Khanna, S. K.; Yen, S. P. S.; Somoano, R. B.; Chaikin, P. M.; Ma, C. L.; Williams, R.; Samson, S. *Phys. Rev. B: Condensed Matter* **1979**, *19*, 655–663, and references therein. (b) Isett, L. C. *Ibid.* **1978**, *18*, 439–447, and references therein. (c) Smith, D. L.; Luss, H. R. *Acta Crystallogr., Sect. B* **1977**, *B33*, 1744–1749. (d) Buravov, L. I.; Zvereva, G. I.; Kaminskii, V. F.; Rosenberg, L. P.; Khidekel, M. L.; Shibaeva, R. P.; Shchegolev, I. F.; Yagubskii, E. B. *J. Chem. Soc., Chem. Commun.* **1976**, 720–721.

(11) (a) Kámaras, K.; Mihály, G.; Grüner, G.; Jánossy, A. *J. Chem. Soc., Chem. Commun.* **1978**, 974–975. (b) Kamaras, K.; Kertesz, M. *Solid State Commun.* **1978**, *28*, 607–611.

(12) (a) Teitelbaum, R. C.; Ruby, S. L.; Marks, T. J. *J. Am. Chem. Soc.* **1980**, *102*, 3322–3328, and references therein. (b) Teitelbaum, R. C.; Ruby, S. L.; Marks, T. J. *Ibid.* **1979**, *101*, 7568–7573.
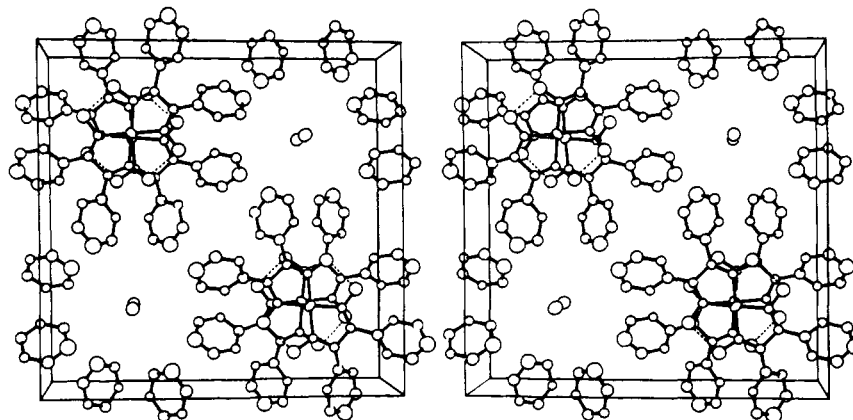
Figure 1. A stereoview of the unit cell of Ni(dpg)$_2$I taken from ref 4a. The *a* axis is horizontal to the right, the *b* axis is vertical from bottom to top, and the *c* axis is toward the reader. The vibrational ellipsoids are drawn at the 50% level, except hydrogen atoms which are drawn arbitrarily small.

Far less is known about the consequences of using bromine as an acceptor in the synthesis of low-dimensional mixed-valent materials. With the exception of the TTF salts where halogen is present as I$^-$ or Br$^-$ and closely interacting with the positively charged donor units,[9d] there is little systematic information on how the degree of partial oxidation and charge-transport facility vary with the nature of the halogen acceptor. Such questions bear upon those features which stabilize the mixed-valence lattice (e.g., acceptor electron affinity[3a]) and the mechanism of charge transport. The latter issue concerns not only the possible effects of acceptor screening but also the actual pathway of conduction. Both donor stacks and polyhalide chains have been discussed as the primary conduction pathway in iodinated low-dimensional materials.[11,13,14] Finally, and unlike the case of polyiodides, there exists no systematic body of structure–spectra criteria which allow ready identification of polybromide structure and hence assessment of the degree of incomplete charge transfer for bromine-doped conductive materials.

We recently reported a detailed study of chemistry, spectroscopy, structure, oxidation state, and charge transport in iodinated nickel and palladium bis(diphenylglyoximates) (M(dpg)$_2$, A).[4a]

A, M = Ni, Pd
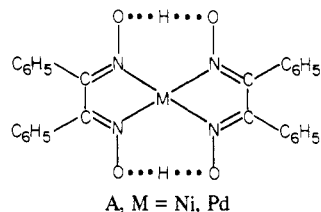
These materials are composed of stacks of partially oxidized, M(dpg)$_2^{0.20+}$ units and parallel chains of disordered I$_5^-$ counterions. The crystal structure of Ni(dpg)$_2$I is shown in Figure 1. We now present a complementary investigation of the effect of substituting bromine for iodine in the M(dpg)$_2$I materials. The bis(diphenylglyoximate) systems are particularly attractive for halogen-substitution studies since M(dpg)$_2$Br[4b,15,16] and M(dpg)$_2$I are virtually isostructural (space group *P4/ncc* with nearly identical unit cell dimensions[16,17]). Furthermore, the halogen chain is spacially well removed from the metal glyoximate core (ca. 7.2 Å). We begin here by developing resonance Raman criteria for the elucidation of polybromide structure, which, beyond the present

system, should be useful in oxidation state characterization of a wide variety of bromine-doped electronic materials. Next, optical spectra are discussed and assigned. Finally, we focus in depth on the transport properties of the M(dpg)$_2$I and M(dpg)$_2$Br$_x$ compounds. If the halogen chains are of primary importance in the conduction pathway, then an appreciable sensitivity of the transport characteristics to the identity of the halogen is expected.[18] It will be seen that single crystals of the brominated M(dpg)$_2$ materials are very similar to the iodinated materials in oxidation state and charge-transport characteristics. This result implicates the M(dpg)$_2$ donor stacks as the major pathway for charge migration. A similar argument has recently been advanced in connection with TTT$_2$I$_x$Br$_{3-x}$ materials, but only *partial* replacement of iodine by bromine could be achieved;[11a] furthermore, the donor and acceptor molecules are not well separated in the TTT–halogen system.[10c]

Experimental Section

All solvents and chemicals were reagent grade. The *o*-dichlorobenzene was dried over Davison 4A molecular sieves. Bis(diphenylglyoximato)-nickel(II) and -palladium(II) were prepared and purified as previously described.[4a] The CsBr$_3$[19a] and (*n*-C$_4$H$_9$)$_4$N$^+$Br$_3^-$[19b] model compounds were prepared according to the literature procedures. Elemental analyses were performed by Ms. H. Beck, Northwestern Analytical Services Laboratory, Micro-Tech Laboratories, or Galbraith Laboratories. All brominated samples were stored in closed vials in a freezer at −20 °C.

Synthesis of Pd(dpg)$_2$Br$_{1.1}$. This complex was prepared by reacting a gravity-filtered, *o*-dichlorobenzene solution of Pd(dpg)$_2$ (ca. 1.8 × 10^{-3} M) at 105 °C with a ca. 24-fold molar excess of Br$_2$. The hot solution was allowed to cool to ambient temperature in the open atmosphere. When the solution had stood at room temperature for a period of 3–5 days, dark needle-like crystals were observed to settle from the solution. The lustrous reddish brown crystals were collected by suction filtration and were washed with hexane until the washings were colorless. By this procedure, the yield of reddish brown needles analyzing as Pd-(dpg)$_2$Br$_{1.13(5)}$ was ca. 40%. By doubling of the concentration of Pd(dpg)$_2$ in the hot solution (ca. 3.6 × 10^{-3} M, ca. 12-fold molar excess of Br$_2$), a mixture of two different crystalline forms was obtained; the reddish brown needles were present as well as brown parallelepipeds, analyzing as Pd(dpg)$_2$Br$_2$·2*o*-C$_6$H$_4$Cl$_2$.

Anal. Calcd for Pd(C$_{14}$H$_{11}$O$_2$N$_2$)$_2$Br$_{1.13}$ (reddish brown needles): C, 49.81; H, 3.28; N, 8.30; Br, 13.37. Calcd for Pd(C$_{14}$H$_{11}$O$_2$N$_2$)$_2$Br$_{1.00}$: C, 50.59; H, 3.34; N, 8.43; Br, 12.02. Found: C, 49.87; H, 3.31; N, 8.41; Br, 13.40 (average of three analyses). Calcd for Pd(C$_{14}$H$_{11}$O$_2$N$_2$)$_2$Br$_2$-

(13) Perlstein, J. H. *Angew. Chem., Int. Ed. Engl.* **1977**, *16*, 519–534.

(14) (a) Huml, K. *Acta Crystallogr.* **1967**, *22*, 29–32. (b) Hadek, V. *J. Chem. Phys.* **1968**, *49*, 5202–5203.

(15) Underhill, A. E.; Watkins, D. M.; Pethig, R. *Inorg. Nucl. Chem. Lett.* **1973**, *9*, 1269–1273.

(16) Foust, A. S.; Soderberg, R. H. *J. Am. Chem. Soc.* **1967**, *89*, 5507–5508.

(17) Ni(dpg)$_2$Br: *a* = 19.51 (6) Å, *c* = 6.72 (2) Å.[16] Ni(dpg)$_2$I: *a* = 19.887 (4) Å, *c* = 6.542 (2) Å.[4a] Pd(dpg)$_2$Br: *a* = 19.78 (6) Å, *c* = 6.57 (2) Å.[16] Pd(dpg)$_2$I: *a* = 20.17 (6) Å, *c* = 6.52 (2) Å.[16]

(18) With the assumption that stoichiometry, crystal structure, and form of polyhalide remain essentially constant in analogous brominated and iodinated materials, then differences in conductivity are expected to arise from the nonequivalent polarizabilities, ionization potentials, electron affinities, and sizes of I and Br, which would lead to vastly different electron correlation and transfer integrals for I and Br in, for example, the one-dimensional Hubbard description.[2] As an illustration, elemental iodine becomes metallic under moderate pressure, whereas elemental bromine does not: (a) Riggleman, B. M.; Drickamer, H. G. *J. Chem. Phys.* **1963**, *38*, 2721–2724; (b) Chao, M. S.; Stenger, V. A. *Talanta* **1964**, *11*, 271–281, and references therein.

(19) (a) Wells, H. L. *Z. Anorg. Chem.* **1892**, *1*, 85–97. (b) Popov, A. I.; Buckles, R. E. *Inorg. Synth.* **1957**, *5*, 167–175.

(o-C$_6$H$_4$Cl$_2$)$_2$ (brown parallelepipeds): C, 46.25; H, 2.91; N, 5.39; Br, 15.39. Found: C, 46.25; H, 2.69; N, 5.44; Br, 17.49.

Infrared data for Pd(dpg)$_2$Br$_{1.1}$ (Nujol mull, cm^{-1}): 3075 (w), 1970 (vw), 1820 (vw), 1595 (mw), 1575 (w), 1515 (w), 1485 (m), 1440 (vs), 1335 (m), 1300 (s), 1275 (m), 1150 (m), 1140 (m), 1070 (w), 1025 (m), 1000 (w), 975 (w), 925 (mw), 880 (s), 840 (vw), 805 (vw), 775 (w), 765 (s), 740 (vs), 690 (vs).

Synthesis of Ni(dpg)$_2$Br$_{1.0}$. This complex was prepared in a manner similar to that of Pd(dpg)$_2$Br$_{1.1}$. An o-dichlorobenzene solution of Ni-(dpg)$_2$ (ca. 2.4 × 10^{-3} M) at 70 °C was gravity filtered, rewarmed to 70 °C, treated with a ca. 29-fold molar excess of Br$_2$, and allowed to cool to ambient temperature in the open atmosphere. Very small, brown, needle-like crystals possessing a metallic green luster formed immediately upon cooling. The crystals were collected by suction filtration and were washed with hexane until the washings were colorless. In this fashion, the yield of brown needles analyzing as Ni(dpg)$_2$Br$_{1.00(5)}$ was ca. 45%. In attempts, similar to the technique used with the corresponding iodides,[4a] to obtain larger crystals by slowly cooling the hot o-dichlorobenzene solutions of Ni(dpg)$_2$ and Br$_2$, a white precipitate and very small amounts of a brown microcrystalline solid were recovered. Thus Ni(dpg)$_2$ is decomposed when being exposed to Br$_2$ at elevated temperatures for extended periods of time.

Anal. Calcd for Ni(C$_{14}$H$_{11}$O$_2$N$_2$)$_2$Br$_{1.00}$: C, 54.50; H, 3.59; N, 9.08; Br, 12.95. Found: C, 54.30; H, 3.60; N, 8.97; Br, 12.94 (average of three analyses).

Infrared data for Ni(dpg)$_2$Br$_{1.0}$ (Nujol mull, cm^{-1}): 3075 (w), 1970 (vw), 1820 (vw), 1600 (mw), 1575 (w), 1525 (mw), 1490 (s), 1445 (vs), 1330 (m), 1295 (s), 1280 (ms), 1155 (m), 1140 (vs), 1100 (mw), 1070 (mw), 1025 (w), 1000 (w), 975 (mw), 930 (m), 900 (ms), 850 (w), 770 (s), 740 (vs), 690 (vs), 670 (mw), 388 (m), 363 (s), 320 (ms), 298 (s), 261 (w), 173 (vs), 110–140 (s).

Raman Measurements. Laser Raman spectra were recorded with Ar$^+$ (4579, 4880, 5145 Å) excitation by using a Spex 1401 monochromator and photon-counting detection. The solid samples were studied in 5- or 12-mm Pyrex sample tubes spinning at 1200 rpm. A 180° back-scattering geometry was employed. A number of scans were made of each sample to check for possible sample decomposition. Spectra were calibrated with the exciting line (ν_0) or laser plasma lines.

Infrared Measurements. Routine infrared spectra were recorded with a Perkin-Elmer Model 267 spectrophotometer. Far-infrared spectra were obtained with a Perkin-Elmer 180 instrument. Samples were studied as Nujol mulls between KBr or polyethylene plates. The far-infrared studies were performed with a thorough and continuous purge of dry nitrogen.

Electronic Spectra. Spectra of solid samples were studied as Nujol mulls between quartz plates in a Cary 17-D spectrophotometer. Several scans were made of each sample to check for possible decomposition.

Electrical Conductivity Measurements. Temperature-dependent dc conductivity measurements were performed on single-crystal specimens of Ni(dpg)$_2$Br$_{1.0}$ and Pd(dpg)$_2$Br$_{1.1}$ by using an automated charge-transport measurement system.[20] The needle geometry of these crystals precluded all measurements other than those along the c axis. In the case of Pd(dpg)$_2$Br$_{1.1}$ typical sample dimensions for the tetragonal needles were 0.50–1.0 mm in length and 0.01–0.05 mm in thickness, whereas for Ni(dpg)$_2$Br$_{1.0}$ the corresponding dimensions were 0.25–0.50 mm in length and ca. 0.005 mm in thickness. Conductivity data were obtained by using the conventional four-probe technique. Due to the small specimen size, considerable care was exercised in the electrode attachment and testing procedures. A special sample holder, which could simultaneously accommodate up to four crystals, was utilized. Each crystal was placed across four 0.025-mm diameter tungsten wires and joined with small droplets of Glydag. Following drying of the Glydag, each crystal was screened at room temperature for any nonohmic or time-dependent behavior and replaced if necessary. The sample holder was then hermetically sealed and placed in the transport measurement apparatus. Bidirectional variable-temperature runs were performed on a large number of crystals with the low-temperature limit determined by sample resistance greater than 10^{12} Ω. Keithley electrometers were utilized for the measurement of sample currents and voltages; a Keithley 225 current source was used to provide the sample current. The data were judged to be meaningful only when reproducible over several runs. The maximum error introduced in conductivity measurements by the determination of sample cross-sectional area is estimated to be no greater than 10%.

No evidence for ionic conduction was observed; passing a steady 10 nA dc current through samples for 2 h did not result in a continuous decline in conductivity which would be expected for carrier depletion by ionic drift. Approximate calculations indicate that complete polarization would occur in less than 2 h for typical samples and currents as low as 10 nA.

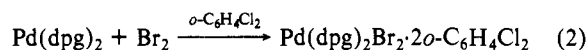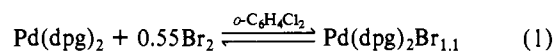(20) Lyding, J. W.; Kannewurf, C. R., manuscript in preparation.

Table I. Resonance Raman Vibrational Data^a for M(dpg)$_2$ and M(dpg)$_2$Br$_x$ (M = Ni, Pd) and Model Polybromide Systems

| compd	$\bar{\nu}$,^{b} cm^{-1}
Ni(dpg)$_2$	418 ms, 113 w(br), 91 vw, 71 vw
Ni(dpg)$_2$Br$_{1.0}$	485 mw(br), 442 vw, 405 vw, 312 vw(br), 247 vs, 158 w
Pd(dpg)$_2$	405 vw, 166 vw, 133 vw, 82 w(sh), 69 vw
Pd(dpg)$_2$Br$_{1.1}$	475 mw(br), 448 vw, 400 vw, 310 vw(br), 244 vs, 156 w
(trimesic acid· H$_2$O)$_{10}$H$^+$Br$_5^-$	265 s, 160 w
Br$_2$ in benzene	306 s
(n-C$_4$H$_9$)$_4$N$^+$Br$_3^-$	301 vw, 264 vw, 251 vw, 191 w, 166 s, 73 w
Cs$^+$Br$_3^-$	342 w(br), 232 m(sh), 215 s, 201 s, 140 m, 125 w, 120 w, 105 w, 78 m, 66 m
PBr$_4^+$Br$_3^-$ ^{c}	251 s, 247 s, 135 m, 94 m

^{a} Polycrystalline samples; Ar$^+$ 5145-A excitation; range recorded: 50–500 cm^{-1}. ^{b} Key: s = strong, m = medium, w = weak, v = very, sh = shoulder, br = broad. ^{c} Data taken from ref 31a for Br$_3^-$ moiety only.

Results and Discussion

Chemistry. The reaction of Pd(dpg)$_2$ with bromine in hot o-dichlorobenzene is found to yield two crystalline products (eq 1 and 2). In the case of relatively dilute solutions (see Exper-

$$Pd(dpg)_2 + 0.55Br_2 \underset{}{\overset{o\text{-}C_6H_4Cl_2}{\rightleftharpoons}} Pd(dpg)_2Br_{1.1} \qquad (1)$$

$$Pd(dpg)_2 + Br_2 \xrightarrow{o\text{-}C_6H_4Cl_2} Pd(dpg)_2Br_2\cdot 2o\text{-}C_6H_4Cl_2 \qquad (2)$$

mental Section for details), lustrous red-brown needles of Pd-(dpd)$_2$Br$_{1.1}$ are isolated. This material has previously been prepared by a somewhat different procedure;[4b] however, in our hands, only the present methodology consistently produces crystals of sufficient dimensions for single crystal, four-probe conductivity measurements. When the concentration of Pd(dpg)$_2$ is increased, brown parallelepipeds of the Pd(IV) complex, Pd(dpg)$_2$Br$_2\cdot 2o$-C$_6$H$_4$Cl$_2$ (eq 2), are also isolated. With use of a procedure similar to the above palladium chemistry, red-brown needles of composition Ni(dpg)$_2$Br$_{1.0}$ can be prepared (eq 3). The bromination

$$Ni(dpg)_2 + 0.50Br_2 \underset{}{\overset{o\text{-}C_6H_4Cl_2}{\rightleftharpoons}} Ni(dpg)_2Br_{1.0} \qquad (3)$$
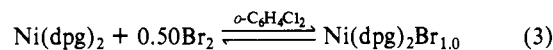
of Ni(dpg)$_2$, using a somewhat different procedure,[4b] has been previously reported, yielding a maximum halogen:metal ratio similar to that observed in the present palladium bromide system. The Ni(dpg)$_2$Br$_{1.0}$ crystals could only be grown in a size marginally suitable for single-crystal conductivity measurements. Attempts to grow crystals by slower cooling of the hot solutions (as was used for the M(dpg)$_2$I materials)[4a] resulted in the complete decomposition of the Ni(dpg)$_2$. For Pd(dpg)$_2$, this procedure resulted in exclusive formation of Pd(dpg)$_2$Br$_2\cdot 2o$-C$_6$H$_4$Cl$_2$. Attempts to grow crystals of either of the M(dpg)$_2$Br$_x$ materials by diffusion techniques were unsuccessful. For the present synthesis, the halogen:metal ratio in brominated Pd(dpg)$_2$ is greater than in the analogous iodinated material by a factor of ca. 13 ± 8%. It will be seen that any greater content of bromine over iodine in M-(dpg)$_2$X compounds can be satisfactorily explained by the smaller spacial demands of the polybromide species (Br$_5^-$) as compared to the analogous polyiodide (I$_5^-$) in lattice channels of essentially constant dimensionality (vide infra).

Resonance Raman Studies. In order to identify the form of bromine present in Ni(dpg)$_2$Br$_{1.0}$ and Pd(dpg)$_2$Br$_{1.1}$ and thus to measure the degree of partial oxidation, we developed resonance Raman spectra–structure criteria analogous to those already employed in this laboratory for polyiodides.[3,4a,21–23] Such criteria

(21) Teitelbaum, R. C.; Ruby, S. L.; Marks, T. J. *J. Am. Chem. Soc.* **1978**, *100*, 3215–3217.

(22) Teitelbaum, R. C.; Ruby, S. L.; Marks, T. J. *J. Am. Chem. Soc.*, in press.

(23) Kalina, D. W.; Stojakovic, D. R.; Teitelbaum, R. C.; Marks, T. J., manuscript in preparation.
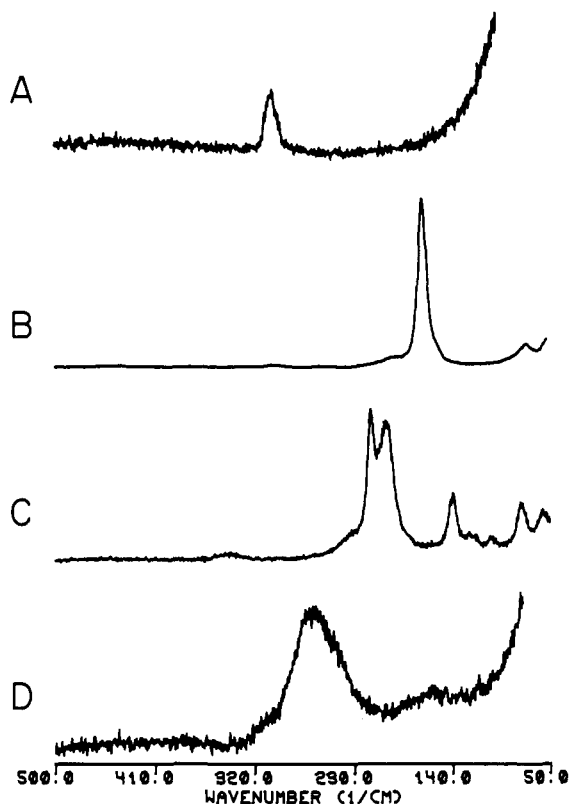
A

B

C

D

```
500.0    410.0    320.0    230.0    140.0    50.0
            WAVENUMBER (1/CM)
```

Figure 2. Resonance Raman spectra (5145-Å excitation) of (A) Br_2 dissolved in benzene, (B) polycrystalline $(n\text{-}C_4H_9)_4N^+Br_3^-$, (C) polycrystalline $Cs^+Br_3^-$, and (D) polycrystalline (trimesic acid·$H_2O)_{10}H^+Br_5^-$.

must be based upon judiciously chosen model compounds of known structure. Figure 2 displays spectra of model compounds containing Br_2 (A), symmetrical ($D_\infty h$) Br_3^- (B), unsymmetrical Br_3^- (C), and symmetrical Br_5^- (D). Spectral data are compiled in

$$\underset{A}{Br\text{-}Br} \qquad \underset{B}{[Br\text{-}Br\text{-}Br]^-} \qquad \underset{C}{[Br\text{-}Br\cdots Br]^-}$$

$$\underset{D}{[Br\text{-}Br\cdots Br\cdots Br\text{-}Br]^-}$$
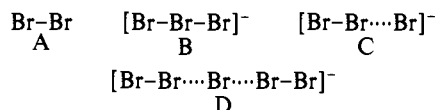
Table I. As in the case of polyiodides, the vibrational spectra of polybromides can be understood in terms of the interaction of Br_2 with species of various electron-donating tendencies. Thus, in the formation of Br_3^-, Br_2 can be viewed as a Lewis acid which interacts with the Lewis base Br^-. Upon complexation of Br_2 with Br^-, Br–Br antibonding molecular orbitals are populated and the Br–Br bond is weakened; thus, the Br–Br distance is increased from 2.29 (1) Å in Br_2[24] to 2.53 (1) Å in $(C_6H_5)_4As^+Br_3^-$,[25] and the resulting force constant is lowered significantly from that in Br_2. In the Raman spectrum of Br_2 in benzene solution (Figure 2A), the fundamental stretching frequency is observed at 306 cm^{-1}. The Raman spectrum of $(n\text{-}C_4H_9)_4N^+Br_3^-$, which has been shown by ^{81}Br nuclear quadrupole resonance[26] spectroscopy to contain symmetrical Br_3^- units (i.e., equal Br–Br distances), is shown in Figure 2B. The actual Br–Br stretching frequency in Br_3^- is given by the average of the symmetrically (166 cm^{-1}) and the antisymmetrically (191 cm^{-1})[27] coupled normal modes,[23] i.e., 179 cm^{-1}; hence, the stretching force constant (0.94 mdyn/Å)[28] has been lowered appreciably from that in Br_2 (2.46 mdyn/Å).[28] In CsBr$_3$, the Br_3^- ions have been distorted by crystal forces, and Br–Br distances of 2.44 (1) and 2.70 (1) Å are observed.[29] Two Br–Br

stretching modes at 208 cm^{-1} (further split by small solid state effects)[27] and 140 cm^{-1} are observed in the Raman spectrum of $CsBr_3$ (Figure 2C). Even greater distortion of the Br_3^- ion has been found in the unusual structure of $PBr_4^+Br_3^-$, which exhibits grossly different tribromide ion Br–Br distances of 2.39 (1) and 2.91 (1) Å.[30] The Raman active Br–Br stretching modes for the Br_3^- ion in $PBr_4^+Br_3^-$ have been observed at 249 and 135 cm^{-1}.[31] The Raman spectrum of the bromine analogue of (trimesic acid·$H_2O)_{10}H^+I_5^-$ (which contains chains of linear I_5^- ions)[4a,32] is displayed in Figure 2D. This material is isomorphous with (trimesic acid·$H_2O)_{10}H^+I_5^-$, and the presence of Br_5^- ions is inferred.[33] It is significant to note that in all instances studied to date, polyiodides and polybromides of the same counterion have the same type of structure.[3a] The intense "Br_2" Br–Br scattering at 265 cm^{-1} in (trimesic acid·$H_2O)_{10}H^+Br_5$ (analogous to the 160-cm^{-1} band in (trimesic acid·$H_2O)_{10}H^+I_5$[4a]) can be explained in terms of the Lewis base Br^- distributing electron density between two Lewis acid Br_2 units; hence, to first order the Br–Br force constant in (trimesic acid·$H_2O)_{10}H^+Br_5$ is expected to be smaller than in Br_2 but larger than in $(n\text{-}C_4H_9)_4N^+Br_3$. The weak scattering at 160 cm^{-1} may be attributed to a symmetric stretching mode which is predominantly $Br_2 \leftarrow Br \rightarrow Br_2$ in character. A similar band at 107 cm^{-1} was observed in the I_5 system.[4a] Alternatively, this transition may be a Raman active π_g bending mode which is also predicted by the selection rules for $D_{\infty h}$ Br_5. The relative intensities of the bands in the Raman spectrum of (trimesic acid·$H_2O)_{10}H^+Br_5^-$ are insensitive to the laser excitation wavelength between 4579 and 5145 Å.

The solid-state resonance Raman spectra of $Ni(dpg)_2Br_{1.0}$ and $Pd(dpg)_2Br_{1.1}$ are presented in Figure 3, and numerical data are tabulated in Table I. The spectra of $Ni(dpg)_2$ and $Pd(dpg)_2$ are displayed elsewhere.[4a] Intense Raman scattering at ca. 245 cm^{-1} and weaker scattering at ca. 157 cm^{-1} is observed in the spectra of both brominated complexes. The overtone and combination bands of these two transitions are also present at ca. 311 (w) (2 × 157), 402 (w) (157 + 245), and 480 (w) (2 × 245) cm^{-1}. The $M(dpg)_2I$ materials display a transition near 157 cm^{-1} (at 160 cm^{-1}) which was assigned to a polyiodide vibration.[4a] That any coincidence or near coincidence with the present 157-cm^{-1} band is fortuitous (and not arising from the $M(dpg)_2^{\delta+}$ moiety) is further confirmed by the presence of the 157 + 245 combination band in the $M(dpg)_2Br_x$ materials. Clearly, the 157-cm^{-1} scattering is associated with a polybromide species. In addition, the presence of the combination band assures that the structures giving rise to the 245- and 157-cm^{-1} bands are in close spacial proximity (i.e., they are not due to different compounds). In the $M(dpg)_2I$ materials, weak Raman transitions due to the $M(dpg)_2^{0.2+}$ units were assigned at 442 cm^{-1} (M = Ni) and at 448 cm^{-1} (M = Pd). It is interesting to note that these "markers" appear to be present at essentially the same energies in the brominated analogues discussed here.

As demonstrated in Figure 4, the relative intensities of the polybromide spectral features in the resonance Raman spectrum of $Ni(dpg)_2Br_{1.0}$ are not particularly sensitive to the laser excitation wavelength between 4579 and 5145 Å. Attempts to obtain further vibrational information on the polybromide species in these materials by far-infrared spectroscopy have been unsuccessful due to the presence of intense $M(dpg)_2$-centered modes in this region.

The resonance Raman data allow immediate rejection of Br_2 and symmetrical Br_3^- as major species present in $Ni(dpg)_2Br_{1.0}$ and $Pd(dpg)_2Br_{1.1}$. Although the results on (trimesic acid·$H_2O)_{10}H^+Br_5^-$ argue strongly for the Br_5^- formulation, the similarity of chromophores in Br_5^- (D) and highly distorted Br_3^- (C)

(24) "Handbook of Chemistry and Physics", 57th ed.; CRC Press: Cleveland, Ohio, 1976-1977; p F-216.

(25) Ollis, J.; James, V. J.; Ollis, D.; Bogaard, M. P. *Cryst. Struct. Commun.* **1976**, *5*, 39-42.

(26) Kume, Y.; Nakamura, D. *J. Magn. Reson.* **1976**, *21*, 235-240.

(27) Gabes, W.; Gerding, H. *J. Mol. Struct.* **1972**, *14*, 267-279.

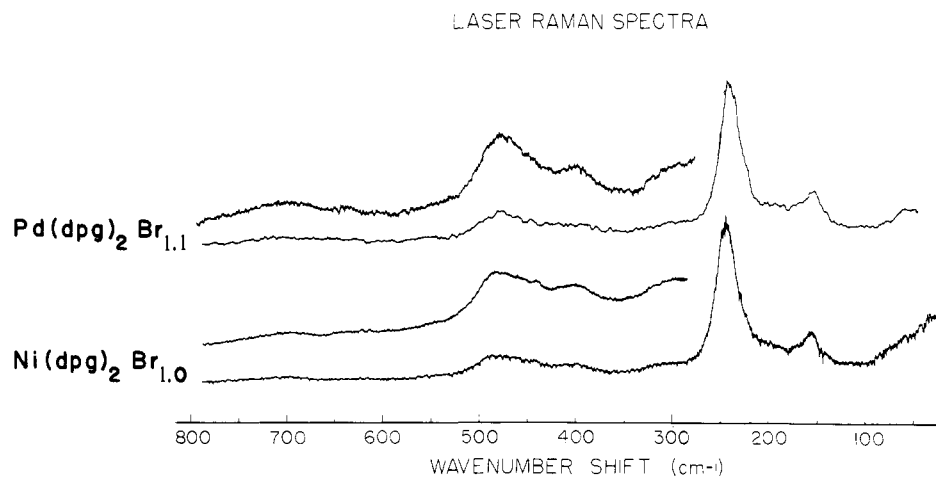(28) Gabes, W.; Elst, R. *J. Mol. Struct.* **1974**, *21*, 1-5.

(29) Breneman, G. L.; Willett, R. D. *Acta Crystallogr., Sect. B* **1969**, *B25*, 1073-1076.

(30) Breneman, G. L.; Willett, R. D. *Acta Crystallogr.* **1967**, *23*, 467-471.

(31) (a) Gabes, W.; Gerding, H. *Recl. Trav. Chim. Pays-Bas* **1971**, *90*, 157-164. (b) The band at 249 cm^{-1} is split to 247 and 251 cm^{-1} by small solid-state effects.[31a]

(32) Herbstein, F. H.; Kapon, M. *Acta Crystallogr., Sect. A* **1972**, *A28*, S74, and private communication.

(33) Herbstein, F. H.; Kapon, M.; Reisner, G. M. *Proc. R. Soc. London, Ser. A* in press.

LASER RAMAN SPECTRA

Figure 3. Resonance Raman spectra (5145-Å excitation, polycrystalline samples) of $Pd(dpg)_2Br_{1.1}$ and $Ni(dpg)_2Br_{1.0}$.

Table II. Calculated Vibrational Stretching Frequencies for Br_2, Symmetric Br_3^-, and Asymmetric Br_3^-, Using Equations 4 and 5[a]

$X_2^{b,c}$

$(\nu_I)_{obsd}$,[d] cm^{-1}	$(\nu_{Br})_{obsd}$, cm^{-1}	N in eq 4	$\nu_{Br} = (\nu_I)_{obsd} \times (\nu_{Br})_{calcd}/(\nu_I)_{calcd}$, cm^{-1}
209^e	306^f	1	316
		0.5	310

Symmetric $X_3^{-g,h}$

$(\nu_I)_{obsd}$, cm^{-1}	$(\nu_{Br})_{obsd}$, cm^{-1}	N in eq 4	$f_{11(I)}^i$	$f_{11(Br)}^i$	$\nu_{Br} = (\nu_I)_{obsd} \times (\nu_{Br})_{calcd}/(\nu_I)_{calcd}$, cm^{-1}
118, $145^{e,j}$	166, $191^{f,j}$	1	$0.36f_1$	$0.42f_1$	178, 205
		0.5	$0.36f_1$	$0.42f_1$	175, 200
		0.4	$0.36f_1$	$0.42f_1$	173, 199
		0.3	$0.36f_1$	$0.42f_1$	170, 196

Asymmetric $X_3^{-k,l}$

$(\nu_I)_{obsd}$, cm^{-1}	$(\nu_{Br})_{obsd}$, cm^{-1}	N_1, N_2 in eq 4	$f_{12(I)}^i$	$f_{12(Br)}^i$	$\nu_{Br} = (\nu_I)_{obsd} \times (\nu_{Br})_{calcd}/(\nu_I)_{calcd}$, cm^{-1}
99, $146^{e,j}$	140, $208^{f,j}$	0.5, 0.5	0.25	0.34	142, 210
		0.5, 0.2	0.25	0.34	138, 207
		0.4, 0.2	0.25	0.34	138, 205

[a] In eq 4, the electronegativities, χ, used to calculate force constants were 2.5 for I and 2.8 for Br; see ref 39a, p 115. [b] Bond lengths, d, for eq 4 were obtained from ref 24. [c] Frequencies $(\nu)_{calcd}$ were calculated from $\lambda = 4\pi^2\nu^2 = f/\mu$, where μ is the reduced mass. [d] All frequencies given are in cm^{-1}. [e] Reference 4a. [f] This work. [g] Bond lengths were obtained from ref 25 and 39c. [h] Frequencies $(\nu)_{calcd}$ were calculated from the general valence force field equations given in ref 36a. [i] Interaction constants were taken from ref 28; units are mdyn/Å. [j] Reference 27. [k] Bond lengths were obtained from ref 29 and 39c. [l] Frequencies $(\nu)_{calcd}$ were calculated from the general valence force field equations given in ref 36b.

warrants further discussion as to how, in general, such species may be differentiated. To begin with, the reasons for which symmetrical trihalide ions distort have been discussed at length.[34] Invariably the driving force for distortion is a spacially and electrostatically unsymmetrical environment; typically the trihalide is caused to distort by interaction with a proximate cation. In the $M(dpg)_2X$ structure (Figure 1) the halogen atoms are in an axially symmetric and nonpolar environment (the "tunnel" is lined with aromatic C–H residues). Thus, the driving force for severe Br_3^- distortion is not evident in the present case; the presence of such a species appears to be incompatible with the structural environment.

We now show that it is possible to predict the Br_5^- Raman spectrum from the corresponding I_5^- spectrum (or, indeed, the spectrum of any simple polybromide from that of the corresponding polyiodide) and that the result is in good agreement with

the observed $M(dpg)_2Br$ spectrum. Stretching force constants in small molecules can be predicted with reasonable accuracy by using the established empirical approach of Gordy[35] (eq 4). Here

$$f = 1.67N\left(\frac{\chi_A\chi_B}{d^2}\right)^{3/4} + 0.30 \qquad (4)$$

for diatomic oscillator AB, N is the bond order, d is the bond distance, and χ_A and χ_B are electronegativities of atoms A and B, respectively. To minimize the uncertainties in N and χ and to take full advantage of the existing polyiodide data, we propose the use of eq 5 where the polybromide frequency can be related

$$\nu_{Br} = (\nu_I)_{obsd}(\nu_{Br})_{calcd}/(\nu_I)_{calcd} \qquad (5)$$

to frequencies calculated (calcd) from eq 4 and the experimental frequency of the analogous polyiodide (obsd). Confidence in this

(34) (a) Rundle, R. E. *Acta Crystallogr.* **1961**, *14*, 585–589. (b) Brown, R. D.; Nunn, E. K. *Aust. J. Chem.* **1966**, *19*, 1567–1576. (c) Migchelsen, T.; Vos, A. *Acta Crystallogr.* **1967**, *22*, 812–815.

(35) (a) Kugimiya, K.; Steinfink, H. *Inorg. Chem.* **1968**, *7*, 1762–1770. (b) Wells, A. F. "Structural Inorganic Chemistry", 3rd ed.; Oxford University Press: London, 1962; p 64. (c) Gordy, W. *J. Chem. Phys.* **1946**, *14*, 305–320.

Table III. Calculated Raman-Active Vibrational Stretching Frequencies for $D_{\infty h}$ Br_5^-, Using Equations 4 and 5[a,b]

$(\nu_{I_5^-})$obsd,[c] cm^{-1}	$(\nu_{Br_5^-})$obsd,[d] cm^{-1}	N_R, N_r in eq 4	d_R, d_r in Br_5^-, Å	f_{rr}[e]		f_{Rr},[f] mdyn/Å		$\nu_{Br_5^-} = (\nu_{I_5^-})$obsd × $(\nu_{Br_5^-})$calcd/ $(\nu_{I_5^-})$calcd, cm^{-1}
				I	Br	I	Br	
104,[h] 162[i]	157, 245	1, 0.5	2.38, 2.82	$0.36f_r$	$0.42f_r$	0.25	0.34	154, 240
		1, 0.5	2.38, 2.82	$0.36f_r$	$0.42f_r$	0.15	0.20	147, 240
		1, 0.5	2.38, 2.82	$0.36f_r$	$0.42f_r$	0.35	0.47	154, 240
		1, 0.5	2.38, 2.82	$0.50f_r$	$0.58f_r$	0.25	0.34	155, 240
		1, 0.5	2.38, 2.82	$0.50f_r$	$0.58f_r$	0.35	0.47	155, 241
		0.7, 0.3	2.38, 2.82	$0.36f_r$	$0.42f_r$	0.25	0.34	151, 237
		1, 0.5	2.37, 2.83	$0.36f_r$	$0.42f_r$	0.25	0.34	154, 241
		1, 0.5	2.36, 2.84	$0.36f_r$	$0.42f_r$	0.25	0.34	154, 241
		1, 0.5	2.35, 2.85	$0.36f_r$	$0.42f_r$	0.25	0.34	154, 242
		1, 0.5	2.34, 2.86	$0.36f_r$	$0.42f_r$	0.25	0.34	153, 242
		1, 0.5	2.33, 2.87	$0.36f_r$	$0.42f_r$	0.25	0.34	153, 243
		1, 0.5	2.28, 2.92	$0.36f_r$	$0.42f_r$	0.25	0.34	151, 246
		1, 0.5	2.39, 2.81	$0.36f_r$	$0.42f_r$	0.25	0.34	153, 240
		1, 0.5	2.40, 2.80	$0.36f_r$	$0.42f_r$	0.25	0.34	153, 239
		1, 0.5	2.41, 2.79	$0.36f_r$	$0.42f_r$	0.25	0.34	153, 238
		1, 0.5	2.42, 2.78	$0.36f_r$	$0.42f_r$	0.25	0.34	154, 238
		1, 0.5	2.43, 2.77	$0.36f_r$	$0.42f_r$	0.25	0.34	155, 238
		1, 0.5	2.48, 2.72	$0.36f_r$	$0.42f_r$	0.25	0.34	155, 235

[a] In eq 4, the electronegativities, χ, used to calculate force constants were 2.5 for I and 2.8 for Br; see ref 39a, p 115. [b] Br–Br bond lengths used in eq 4 to calculate force constants for the Br_5^- ion were obtained by multiplying the I–I bond lengths in (trimesic acid·$H_2O)_{10}H^+I_5^-$ (ref 32 and 4a) by 0.87 (see text). [c] Raman data for (trimesic acid·$H_2O)_{10}H^+I_5^-$ were taken from ref 4a; all frequencies given are in cm^{-1}. [d] Raman data for $M(dpg)_2Br_x$ materials, M = Ni, Pd; see Table I. These values represent the averages of the Raman data for M = Ni and M = Pd. [e] Interaction constants were taken from ref 28 and then were allowed to vary. Typical results are given. [f] Interaction constants were taken from ref 28 and then were allowed to vary. Typical results are given. [g] Frequencies (ν)calcd were calculated from the general valence force field equation given in ref 40 (see text). [h] In $M(dpg)_2I$, this band is observed at 107 (M = Ni) and 104 (M = Pd) cm^{-1} (ref 4a). [i] In $M(dpg)_2I$, this band is observed at 162 (M = Ni) and 160 (M = Pd) cm^{-1} (ref 4a).
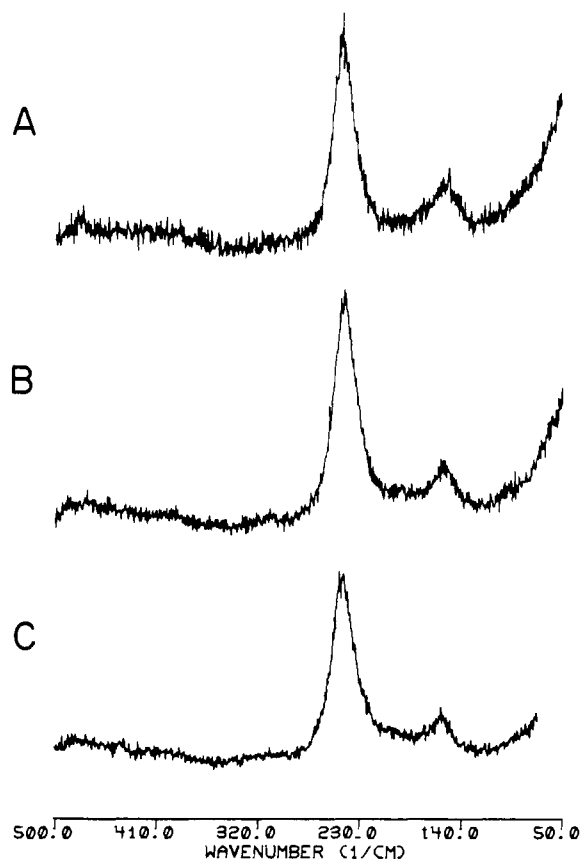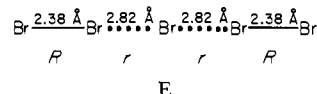

Figure 4. Raman spectra of $Ni(dpg)_2Br_{1.0}$ (polycrystalline sample) with (A) 4579-Å excitation, (B) 4880-Å excitation, and (C) 5145-Å excitation.

approach is affirmed by the calculated parameters for Br_2 and Br_3^- in Table II, which are derived from eq 4 and 5, literature data for I_2 and I_3^-, and, in the case of X_3^-, the appropriate gen-

eralized valence force field equations[36] (estimating the stretch–stretch interaction constant by an established method[28]). The results are in excellent agreement with experiment and, importantly, relatively insensitive to choice in N.[37] Thus, it should be possible to predict the Br_5^- vibrational spectrum beginning with I_5^- data and a reasonable estimate of the Br_5^- molecular structure.

The Br_5^- metrical parameters can be estimated by noting the near constancy of the following Br:I distance ratios:[39] covalent radii, 0.86;[39a] ionic radii, 0.83;[39b] halogen–halogen distance in the symmetrical trihalide, 0.87;[39c] and halogen–halogen distance in the distorted trihalide (with the same counterion), 0.86 and 0.89.[39d] The average of these Br:I distance ratios, 0.87 ± 0.01, multiplied by the known I_5^- distances,[4a,32] yields the pentabromide structure shown below (E). These metrical parameters for I_5^- and Br_5^-

$$Br\,\overset{2.38\ \text{Å}}{\text{---}}\,Br\,\overset{2.82\ \text{Å}}{\cdots}\,Br\,\overset{2.82\ \text{Å}}{\cdots}\,Br\,\overset{2.38\ \text{Å}}{\text{---}}\,Br$$
$$R\qquad r\qquad r\qquad R$$

E

were next used in eq 4 to calculate stretching force constants. Nearest-neighbor stretch–stretch interaction constants (f_{Rr}, f_{rr}) in the secular equation for a linear pentaatomic molecule[40] were

(36) (a) For symmetric X_3^-, the generalized valence force field equations are $\nu_1 = (1/2\pi)[(f_1 + f_{11})/m_x]^{1/2}$ and $\nu_3 = (1/2\pi)[3(f_1 - f_{11})/m_x]^{1/2}$. See: Herzberg, G. N. "Infrared and Raman Spectra of Polyatomic Molecules"; Van Nostrand: New York, 1945; pp 153–154. (b) For unsymmetrical X_3^-, the generalized valence force field equations are $\lambda_1 + \lambda_3 = 4\pi^2(\nu_1^2 + \nu_3^2) = (2m_x)(f_1 + f_2 - f_{12})$ and $\lambda_1\lambda_3 = 16\pi^4\nu_1^2\nu_3^2 = (3/m_x^2)(f_1f_2 - f_{12}^2)$. See: Richardson, W. S.; Wilson, E. B., Jr. *J. Chem. Phys.* **1950**, *18*, 694–696.

(37) Previous bond order determinations, based upon experimental spectroscopic data[28] and upon molecular orbital calculations,[38] indicate that $N = 1$ for $X_2^{28,35c}$ and $N = 0.38^{28} - 0.71^{38}$ for X_3^- are reasonable values.

(38) (a) Datta, S. N.; Ewig, C. S.; Van Wazer, J. R. *J. Mol. Struct.* **1978**, *48*, 407–416. (b) Gabes, W.; Nijman-Meester, M. A. M. *Inorg. Chem.* **1973**, *12*, 589–592. (c) Wiebenga, E. H.; Kracht, D. *Ibid.* **1969**, *8*, 738–746.

(39) (a) Cotton, F. A.: Wilkinson, G. "Advanced Inorganic Chemistry", 3rd ed.; Wiley: New York, 1972; p 117. (b) Shannon, R. D. *Acta Crystallogr., Sect. A.* **1976**, *A32*, 751–767. (c) Reference 25 and Runsink, J.; Swen-Walstra, S.; Migchelson, T. *Acta Crystallogr., Sect. B* **1972**, *B28*, 1331–1335. (d) Reference 29 and Runsink, J.; Swen-Walstra, S.; Migchelson, T. *Ibid.* **1972**, *B28*, 1331–1335.

7860 *J. Am. Chem. Soc., Vol. 102, No. 27, 1980*

Kalina et al.

Table IV. Ratios of the High- to Low-Energy Vibrational Stretching Transitions[a] in Polyhalides

species	X	$(\nu)_{high}$, cm^{-1}	$(\nu)_{low}$, cm^{-1}	$(\nu)_{high}/(\nu)_{low}$
sym X$_3^-$	I	145[b]	118[b]	1.23
	Br	191[c]	166[c]	1.15
asym X$_3^-$	I	146[b]	99[b]	1.47
X$_5^-$	Br	208[c]	140[c]	1.48
	I	162[d]	104[d]	1.56
		162[e]	107[e]	1.51
		160[f]	104[f]	1.54
	Br	247[g]	158[g]	1.56
		244[h]	156[h]	1.56
		265[i]	160[i]	1.65
extremely distorted X$_3^-$	Br	249[j]	135[j]	1.84

[a] Stretching frequencies given are in cm^{-1}. [b] References 4a and 27. [c] Reference 27 and this work. [d] Reference 4a; data for (trimesic acid·H$_2$O)$_{10}$H$^+$I$_5^-$. [e] Reference 4a; data for Ni(dpg)$_2$I. [f] Reference 4a; data for Pd(dpg)$_2$I. [g] This work; data for Ni(dpg)$_2$Br$_{1.0}$. [h] This work; data for Pd(dpg)$_2$Br$_{1.1}$. [i] This work; data for (trimesic acid·H$_2$O)$_{10}$H$^+$Br$_5^-$. [j] Reference 31.

approximated as for the trihalides,[28] and nonnearest-neighbor interaction constants (f_{RR}, f_{Rr_2}) were set equal to zero. It can be seen in Table III that the agreement between experimental Br$_5^-$ frequencies and those predicted from eq 5 by using the (trimesic acid·H$_2$O)$_{10}$H$^+$I$_5^-$ Raman data[4a] is very good; agreement is also good when the M(dpg)$_2$I spectral data are used as a starting point (Table III). The results are not particularly sensitive to reasonable choice of *N*, interaction constants, or bond distances.

A complementary way in which to assess the congruency between the polyiodide and polybromide vibrational data is by examining the ratio of the high to low-energy Raman scattering transitions. As can be seen in Table IV, the pentahalide ratios fall within a relatively narrow range, distinct from all the other species tabulated. The distorted tribromides fall into two classes. The moderately asymmetric species (e.g., CsBr$_3$) have slightly smaller frequency ratios than Br$_5^-$, but the actual frequencies are substantially lower. The latter effect no doubt arises from the greater concentration of negative charge on the single Br$_3^-$ chromophore in tribromide (similar effects are evident in molecular orbital calculations,[38] [129]I Mössbauer isomer shifts,[4a] and nuclear quadrupole coupling constants[4a,41]). The result of the more localized negative charge is a greater reduction in bond orders and force constants than in the pentahalide (lower electronegativities in terms of eq 4). The second class of distorted tribromides, those evidencing extreme distortion, is represented by PBr$_4^+$Br$_3^-$; here the high frequency stretch approaches that of Br$_5^-$ (becomes more "Br$_2$-like"). However, the low-energy stretching mode of this Br$_3^-$ ion is considerably below that of Br$_5^-$. Again the more concentrated negative charge explains this effect. A large, positive stretch–stretch interaction constant, f_{rr}(E), would further raise the energy of the low frequency mode in Br$_5^-$.

To summarize, the form of bromine in the M(dpg)$_2$Br materials, as deduced from our resonance Raman data employing several lines of argument, can be assigned predominantly, if not exclusively, to Br$_5^-$. Thus, we estimate the charges on the metal–ligand units as Ni(dpg)$_2^{0.20(2)+}$ and Pd(dpg)$_2^{0.22(2)+}$.

Electronic Absorption Spectra. The electronic absorption spectra of the M(dpg)$_2$ and M(dpg)$_2$Br$_x$ systems, M = Ni, Pd, are presented in Figure 5A–D, and the data are compiled in Table V. Upon bromination the lowest energy bands at 515 nm in Ni(dpg)$_2$ and 445 nm in Pd(dpg)$_2$ are shifted to lower energies,

Figure 5. Electronic absorption spectra (polycrystalline samples as Nujol mulls) of (A) Pd(dpg)$_2$Br$_{1.1}$, (B) Pd(dpg)$_2$, (C) Ni(dpg)$_2$Br$_{1.0}$, (D) Ni-(dpg)$_2$, and (E) (trimesic acid·H$_2$O)$_{10}$H$^+$Br$_5^-$.

Table V. Electronic Spectral Data[a] for M(dpg)$_2$ and M(dpg)$_2$Br$_x$ (M = Ni, Pd) as Nujol Mulls

compd	abs, nm ($\times 10^3$ cm^{-1})	compd	abs, nm ($\times 10^3$ cm^{-1})
Ni(dpg)$_2$	285 (35.1)	Pd(dpg)$_2$	235 (42.6)
	335 sh (29.9)		278 (36.0)
	372 sh (26.9)		365 (27.4)
	435 (23.0)		445 (22.5)
	515 (19.4)	Pd(dpg)$_2$Br$_{1.1}$	235 (42.6)
Ni(dpg)$_2$Br$_{1.0}$	285 (35.1)		280 (35.7)
	335 sh (29.9)		360 (27.8)
	375 sh (26.7)		455 (22.0)
	440 (22.7)		500 (20.0)
	485 (20.6)		600 sh (16.7)
	520 (19.2)		
	570 sh (17.5)		
	650 sh (15.4)		

[a] Range recorded: 200–2100 nm; sh = shoulder.

520 and 455 nm, respectively. This is consistent with the assignment of these features to intramolecular $nd_{z^2} \rightarrow (n + 1)p_z$ transitions which borrow intensity from intermolecular metal–metal charge-transfer transitions.[42] The energies of such solid-state electronic transitions in stacked d^8 palladium and nickel bis(glyoximates) have been demonstrated to be polarized parallel to the chain direction[42] and to be sensitive to intrastack metal–metal separation.[42,43] Thus, upon bromination of the M(dpg)$_2$

(40) For symmetric X$_5^-$, the generalized valence force field equation for the Raman-active stretching frequencies is $\lambda^2 - \lambda[(1/m_x)(2f_R + f_{RR} + f_r + f_{rr} - 2f_{Rr_1} - 2f_{Rr_2})] + (1/m_z^2)[(f_R - f_{RR})(f_r + f_{rr}) - (f_{Rr_1} + f_{Rr_2})^2] = 0$, where $\lambda_+ = 4\pi^2\nu_1^2$ and $\lambda_- = 4\pi^2\nu_2^2$. See: Smith, W. H.; Leroi, G. E. *J. Chem. Phys.* **1966**, *45*, 1767–1777; Long, D. A.; Murfin, F. S.; Williams, R. L. *Proc. R. Soc. London, Ser. A* **1954**, *A223*, 251–266.

(41) (a) Breneman, G. L.; Willett, R. D. *J. Phys. Chem.* **1967**, *71*, 3684–3686. (b) Lucken, E. A. C. "Nuclear Quadrupole Coupling Constants"; Academic Press: New York, 1969; Chapter 12.
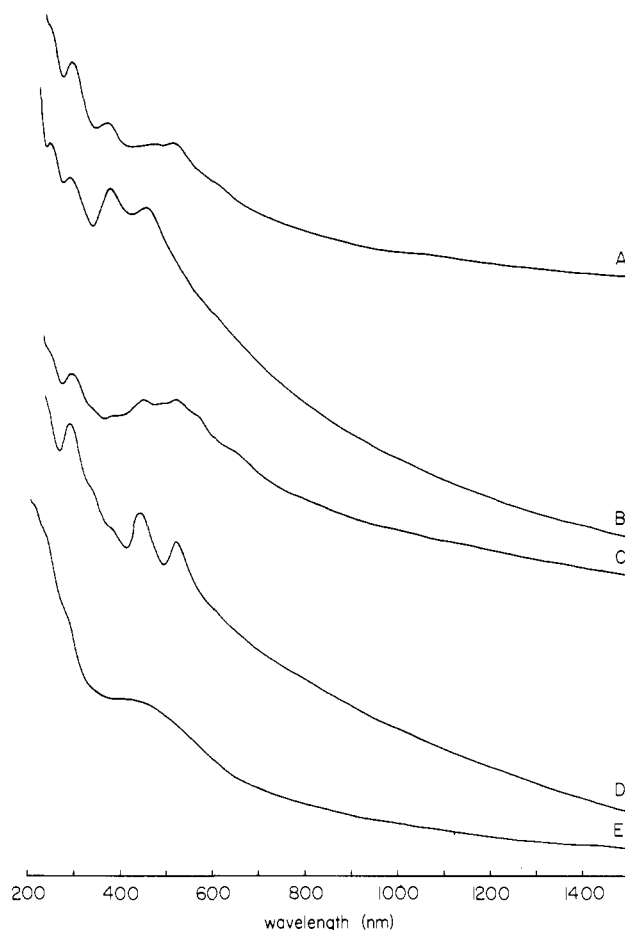
(42) (a) Anex, B. G. *ACS Symp. Ser.* **1974**, *No. 58* 276–300. (b) Hara, Y.; Shirotani, I.; Onodera, A. *Solid State Commun.* **1976**, *19*, 171–175. (c) Ohashi, Y.; Hanazaki, I.; Nagakura, S. *Inorg. Chem.* **1970**, *9*, 2551–2556. (d) Nishida, Y.; Kozuka, M.; Nakamoto, K. *Inorg. Chim. Acta* **1979**, *34*, L273–L275.
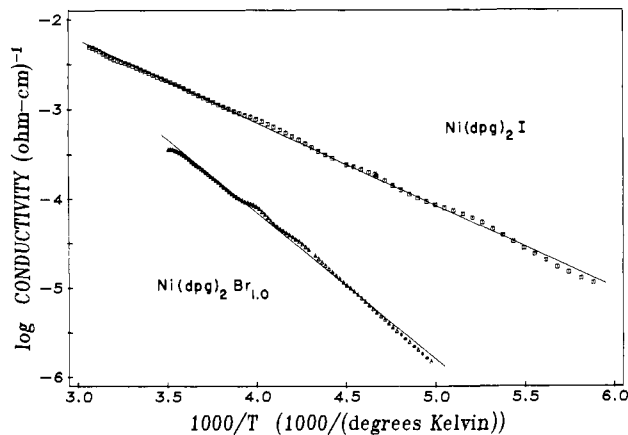
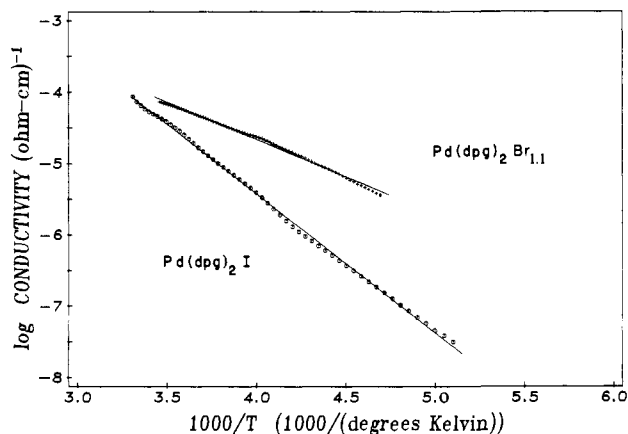**Figure 6.** Electrical conductivity in the crystallographic c direction for typical $Ni(dpg)_2Br_{1.0}$ and $Ni(dpg)_2I$ crystals as a function of temperature.

Figure 7. Electrical conductivity (dc) in the crystallographic c direction for typical $Pd(dpg)_2Br_{1.1}$ and $Pd(dpg)_2I$ crystals as a function of temperature.

materials, the intrastack metal–metal distances are decreased (by 0.20 Å for M = Ni;[4,16] by 0.24 Å for M = Pd[4,16]) and, as anticipated, the low-energy bands are red-shifted. The bands in $M(dpg)_2$ at 435 nm (M = Ni) and 365 nm (M = Pd) can be assigned[42] to intramolecular metal–ligand ($d\pi \rightarrow \pi^*$) transitions and are expected to be rather insensitive to metal–metal separation.[42] In support of metal–ligand origin, the bands are present at essentially the same energy in the $M(dpg)_2I^{4a}$ and $M(dpg)_2Br_x$ materials. An intense, broad, underlying feature is also observed at lower energies (400–550 nm) in the spectra of the $M(dpg)_2Br_x$ materials. A similar, broad absorption centered at 425 nm is evident in the spectrum (Figure 5E) of the Br_5^- chain compound (trimesic acid·$H_2O)_{10}H^+Br_5^-$. Transitions in the region 400–475 nm have also been observed in the solid-state electronic spectra of Br_3^- compounds.[44] Therefore, it is not unreasonable to assign the broad feature in the spectra of the $M(dpg)_2Br_x$ materials to transitions within the polybromide chains, as argued for the corresponding polyiodide systems.[4a] It is these transitions which are doubtless responsible for the resonant enhancement of the polybromide Raman spectra.

Electrical Conductivity. Single-crystal measurements of $Ni(dpg)_2Br_{1.0}$ and $Pd(dpg)_2Br_{1.1}$ conductivity were performed as a function of temperature by the four-probe technique. The thinness of the crystals only permitted transport measurements in the needle direction. Because comparison of $M(dpg)_2Br_x$ and $M(dpg)_2I$ conductivities was a major goal in this investigation, great care

Table VI. Single-Crystal Four-Probe Electrical Conductivity Data for Partially Oxidized Metal Bis(diphenylglyoximates)

material	dc conductivity[a] at 295 K, $(\Omega$ cm)$^{-1} \times 10^4$	Δ,[b] eV	$c/2$,[c] Å
$Pd(dpg)_2Br_{1.1}$	0.8–1.5	0.208 ± 0.002	3.28 (1)
$Pd(dpg)_2I$	0.2–0.8	0.388 ± 0.002	3.26 (1)
$Ni(dpg)_2Br_{1.0}$	3.8–9.1	0.327 ± 0.002	3.36 (1)
$Ni(dpg)_2I$	18–55	0.184 ± 0.0008	3.271 (2)
$Pd(dpg)_2$[d]	$\langle 8 \times 10^{-5}$		
$Ni(dpg)_2$[d]	$\langle 8 \times 10^{-5}$		

[a] Range given for specimens examined. [b] From least-squares fit to eq 6. [c] Interplanar separation; see ref 17. [d] From ref 4a.

was taken to ensure that specimens and contacts were of the highest possible quality.

In Figures 6 and 7 are shown representative variable-temperature conductivity data comparing the iodinated and brominated complexes of nickel (Figure 6) and palladium (Figure 7). The data adhere closely to a linear ln σ vs. $1/T$ relationship over the temperature range investigated. As in the case of the $M(dpg)_2I$ materials,[4a] the data could be fit by the method of least squares to a thermal activation model (eq 6) with the parameters compiled in Table VI.

$$\sigma = \sigma_0 e^{-\Delta/kT} \tag{6}$$

Several features are obvious upon viewing the conductivity data. First, as in the case of iodine doping,[4a] bromination has brought about a very large increase (ca. 10^7–10^8) in the metal bis(diphenylglyoximate) charge-transport capacity. Second, there is no clear-cut evidence that bromination produces materials with significantly and uniformly different charge-transport characteristics than iodination. Thus, although the brominated derivative is perhaps slightly more conductive and has a lower activation energy for conduction in the palladium system, the exactly opposite trend is observed in the nickel system. These results argue against the halogen chains being the principal conduction pathway. As was noted earlier, the iodine-containing chains would be expected, all other factors being equal, to be far more efficient charge carriers than the bromine-containing chains.[18] This expectation is not confirmed by the conductivity data. Indeed, for the nickel and palladium bis(diphenylglyoximates), the effect of changing the halogen is no greater than changing the metal (which is a relatively small effect in this and most other partially oxidized metallomacrocycle systems).[3–8] It is also interesting to note that the nickel complex is somewhat more conductive than the palladium analogue, which was also found for the $M(dpg)_2I$ systems.[4a] Additional evidence for the major conduction pathway being the $M(dpg)_2^{\delta+}$ stacks is derived from thermoelectric power measurements. These will be discussed in detail elsewhere.[45] We note here that for $Ni(dpg)_2I$, $S = +40$ $\mu V/K$, and that for $Pd(dpg)_2Br$, $S = +127$ $\mu V/K$. The positive sign can be taken as evidence for hole conduction,[8b,10a,b,46] and the similarities in the iodide/bromide data again underscore the close congruencies in transport characteristics for the materials with different halogens.

Conclusions

Bromination of $Ni(dpg)_2$ and $Pd(dpg)_2$ yields the partially oxidized materials $Ni(dpg)_2Br_{1.0}$ and $Pd(dpg)_2Br_{1.1}$, in which the predominant, if not exclusive, halogen-containing species is Br_5^-. Resonance Raman spectroscopy represents a powerful tool for the structural identification of polybromides, and simple empirical relationships permit the prediction of polybromide spectra from those of the analogous polyiodides. The degree of $M(dpg)_2$ partial oxidation in the present case (ca. 0.20 (2) +, M = Ni; ca. 0.22 (2) +, M = Pd) is equal to or only slightly greater than that in

(43) (a) Anex, B. G.; Krist, F. K. *J. Am. Chem. Soc.* **1967**, *89*, 6114–6125. (b) Banks, C. V.; Barnum, D. W. *Ibid.* **1958**, *80*, 4767–4772. (c) Basu, G.; Cook, G. M.; Belford, R. L. *Inorg. Chem.* **1964**, *3*, 1361–1368. (d) Zahner, J. C.; Drickamer, H. G. *J. Chem. Phys.* **1960**, *33*, 1625–1628.
(44) Gabes, W.; Stufkens, D. J. *Spectrochim. Acta, Ser. A* **1974**, *A30*, 1835–1841.

(45) Lyding, J. W.; Kannewurf, C. R.; Marks, T. J., manuscript in preparation.
(46) Chaikin, P. M.; Grüner, G.; Shchegolev, I. F.; Yagubskii, E. B. *Solid State Commun.* **1979**, *32*, 1211–1214.

the iodine-doped analogues (0.20+) (a similar observation was made in the case of tetrathiafulvalenium iodides and bromides[9e]). Any differences in M(dpg)$_2$X oxidation states arise from a slightly greater degree of bromine incorporation. In this regard, it is interesting to note that the 0.87 bromine to iodine size relationship mentioned earlier leads to a maximum possible predominance of bromine over iodine of ca. 1.15 in the filling of isostructural lattice tunnels. The transport properties of the M(dpg)$_2$Br compounds do not differ greatly from those of the M(dpg)$_2$I compounds, and

it therefore seems unreasonable that the halogen chains provide the dominant pathway for charge conduction.

Synthesis and Structure Determination of 2-Azabicyclo[2.2.1]hept-2-enes and Their Derivatives. W Effect on Chemical Shifts

Michael E. Jung*[1] and Jerel J. Shapiro

Contribution from the Department of Chemistry, University of California, Los Angeles, California 90024. Received June 5, 1980

Abstract: The Diels–Alder reaction of vinyl acetate **6** and 2,3,4,5,5-pentachloro-1-azacyclopentadiene **2** afforded not the expected 1-azabicyclo[2.2.1]hept-2-ene (**4**) but rather the 2-aza isomer **7**. The cycloaddition occurred via the isomeric diene, 1,3,4,5,5-pentachloro-2-azacyclopentadiene **2′**, which is presumably in equilibrium with the 1-aza isomer at elevated temperatures. Possible reasons for this often observed reluctance of 1-azadienes to undergo cycloaddition are discussed. The regio- and stereochemistry of the acetate group was determined by the chemical shifts and especially the coupling constants in its ^{1}H NMR spectrum. In addition, the structures of the products of reduction of **7** under a variety of conditions were also determined, largely by means of their ^{1}H and ^{13}C NMR, which are discussed in detail. In general, W arrangement between a proton and a chlorine atom (e.g., in the 6-endo and 7-syn positions, respectively) causes a downfield shift of ≃0.15–0.21 ppm. Examination of the NMR spectra of 1-substituted adamantane derivatives indicates that this W effect on chemical shifts is a general one and can be quite large. A possible reason for this effect is discussed. In addition, the presence of a chlorine syn to an exo proton causes a downfield shift of 0.1–0.3 ppm. Finally, reduction of **7** with ethanolic borohydride effected a fragmentation of the bicyclo[2.2.1]heptene system to produce the monocyclic pyrrole **13**.

Introduction

In the course of a project aimed at the total synthesis of indolizidine and pyrrolizidine alkaloids, we required a synthesis of 1-azabicyclo[2.2.1]hept-5-en-3-one (**1**). This amino enone is a
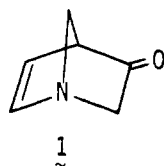
representative of a class of unknown compounds, namely, polycyclic enamino ketones in which the presence of the bridgehead nitrogen eliminates any overlap of the N lone pair with the C–C double bond. A particularly attractive synthetic route to this molecule involved an initial Diels–Alder reaction of 2,3,4,5,5-pentachloro-1-azacyclopentadiene **2** with a monosubstituted olefin. Although the diene **2** has been known for more than 80 years,[2] it was not until 1975 that its first use in Diels–Alder additions was reported. Wong[3] described its addition to several olefins, among which was styrene **3** which reportedly afforded the 3-phenyl-1-azabicyclo[2.2.1]hept-5-ene **4** (eq 1). Based on these results, we initiated a program directed toward the use of **2** in a Diels–Alder-based approach to **1**. Early in our study we were surprised at the unreactivity of certain reduction products of our Diels–Alder adducts and began to question the validity of Wong's

(1)
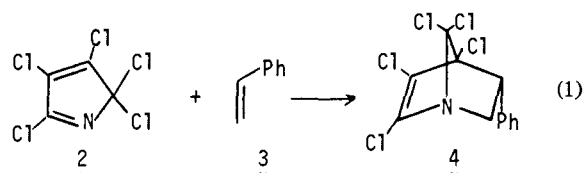
original structure assignment. Very recently Wong[4] has reported a reexamination of the structure of the adduct of **2** and **3** in which an X-ray crystallographic study conclusively confirmed the structure as 2-aza-5-phenylbicyclo[2.2.1]hept-2-ene (**5**). This report prompts us to describe our own work in this area which affirms the propensity of Diels–Alder additions of **2** to proceed via the 2-azadiene isomer **2′**, thereby producing 5-substituted 2-azabicyclo[2.2.1]hept-2-enes.
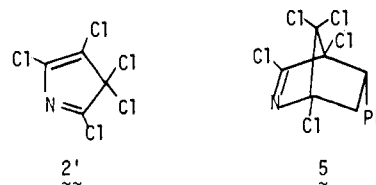
Results and Discussion

With the eventual goal of producing a β-keto amine system such as **1**, we chose to investigate the Diels–Alder addition of vinyl acetate **6** with the pentachloro-1-azacyclopentadiene **2**. Refluxing a solution of **2**, prepared by the method of Mazzara,[2a] in excess

(1) Camille and Henry Dreyfus Teacher-Scholar, 1978–1983; Fellow of the Alfred P. Sloan Foundation. 1979–1981.

(2) (a) Anschutz, R.; Schroeter, G. *Justus Liebigs Ann. Chem.* **1897**, *295*, 86. (b) Mazzara, G. *Gazz. Chim. Ital.* **1902**, *32II*, 28.

(3) Gladstone, C. M.; Daniels, P. H.; Wong, J. L. *J. Org. Chem.* **1977**, *42*, 1375.

(4) Daniels, P. H.; Wong, J. L.; Atwood, J. L.; Canada, L. G.; Rogers, R. D. *J. Org. Chem.* **1980**, *45*, 435.